The Eurasia Proceedings of Science, Technology,
Engineering & Mathematics (EPSTEM)
ISSN: 2602-3199

The Eurasia Proceedings of Science, Technology, Engineering & Mathematics (EPSTEM), 2022

Volume 20, Pages 84-93

ICBAST 2022: International Conference on Basic Sciences and Technology

Theoretical (B3lyp) and Spectroscopic (Ft-Ir, ^{1}h-Nmr and ^{13}c-Nmr) Investigation of 2- Methoxy-6-[(3-(*P*-Methylbenzyl)-4,5-Dihydro-1*h*-1,2,4-Triazol-5-One-4-Yl)-Azomethin]-Phenyl Benzoate

Gul KOTAN
Kafkas University

Haydar YUKSEK
Kafkas University

Abstract: Density functional theory (DFT) is an inexpensive approach used to study the molecular structure, many theoretical properties, biological activities and electronic properties of simple and complex compounds. In this study, the all quantum chemical studies of 2-Methoxy-6-[(3-(p-methylbenzyl)-4,5-dihydro-1*H*-1,2,4-triazol-5-one-4-yl)-azomethin]-phenyl Benzoate molecule were calculated using the DFT(B3LYP) method with 6-311++G(d,p) basis set. For use in all these computational processes, initially the molecule was optimized. Thus, the most stable state of atoms was reached. Then, the calculations of carbon-13 and proton-NMR isotropic shift values were performed in the solvent (DMSO) and gaseous with "the gauge-independent atomic orbital" (GIAO). Infrared (FT-IR) vibration frequency values were calculated from the Veda4f program. The theoretical vibration frequency values were compared with the experimental IR values. Experimental data obtained from the literature. In addition, the electronic properties (chemical hardness and softness, ionization potential (I), electronegativity (χ), electron affinity (A), electrophilic and nucleophilic index), ΔEg energy gap, HOMO-LUMO energies, the geometric properties (bond angle and length), the thermodynamic properties (thermal capacity (CV), entropy (S), thermal energy (E), dipole moment, mulliken atomic charge values, molecular electron potential (MEP), total density and contour surface maps and the total energy of the molecule were determined.

Keywords: 6-31 G(d,p), DFT, DMSO, FT-IR.

Introduction

Schiff bases, which contain a triazole ring containing three nitrogen atoms and carry 1,2,4-triazole, have a specific -C=N- imine group in their structure. The 1,2,4-triazole main structure is involved in the structures of many substances with a wide range of biological activities, including insecticides, antimicrobials (Singla, 2020), antituberculous agents (Aly et al., 2020), anticonvulsants (Kopron et al., 2020), anti-inflammatory agents (Abuo-Rahma et al., 2014), analgesics (Patel et al., 2018) antiasthmatic agents (Gao et al., 2019), antidepressants (Shi et al., 2020). Numerous studies have been conducted on Schiff bases that include 1,2,4-triazole to determine if they may be used in biological (Boy et al., 2021; Yüksek et al., 2018; Kotan et al., 2022; Yüksek et al., 2020, Dharmaraj et al., 2001), chemical (Jin et al., 2018; Kotan et al., 2021) or medicinal applications (Yiğit et al., 2018; Qiao et al., 2011). Also, recently quantum chemical computations have been used to examine the theoretical characteristics of Schiff bases (Kotan et al., 2020; Beytur et al., 2021). The calculation results were compared with the experimental results from the literature (Gürbüz et al., 2021). The computations were done on a computer system utilizing the Gaussian 09W software package, the 6-311G++(d,p) basis sets, and the Hartree-Fock (HF) and density functional theory (DFT) techniques (Frisch et al., 2009). First, the compound was optimized using the 6-31G(d,p) basis set and DFT(B3LYP) technique (Frisch et al., 2009; Wolinski et al., 1990). Then, using the GIAO approach, the values of the ^{13}C/ ^{1}H-NMR isotropic shift were computed (Wolinski et al.,

---

- Selection and peer-review under responsibility of the Organizing Committee of the Conference

1990). IR data definition was done using the veda4f application (Jamroz, 2004). The necessary scala factors are used to scale theoretically computed IR data (Merrich et al., 2007). Theoretical infrared spectrum is used to create scaled DFT values. Additionally, the computer was used to determine the HOMO-LUMO energy, bond lengths, thermodynamic parameters, the E_{LUMO}-E_{HOMO} energy gap (Eg), electronic characteristics, total energy, the dipole moment, MEP analysis, and mulliken charges.

RESULTS AND DISCUSSION

Computational Data

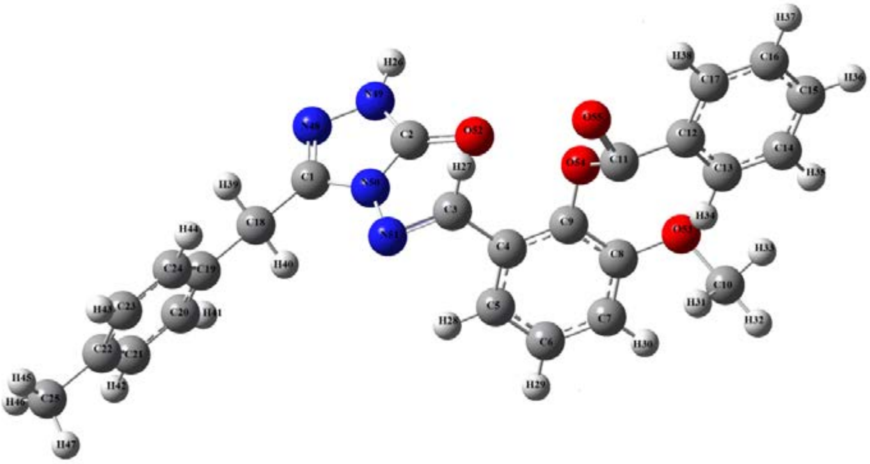

Figure 1. The optimized molecule structure

NMR Data

The GIAO technique from the Gaussian package software was used to conduct all NMR analyses and make visuals.There is a connection between the compound's R-values. B3LYP /6-31G(d,p) (DMSO): ^{1}H: 0.8659; B3LYP/6-31G(d,p) (DMSO): ^{13}C: 0.9939. The Table 1/ Figure 2 showed these compound values. Experimental and theoretical data were compared and a linear correlation was found in ^{13}C NMR while a deviation was observed in ^{1}H-NMR. This was due to the N-H acidic proton.

Table 1. The experimental and theoretical ^{13}C and ^{1}H-NMR chemical shift data

No	Experimental	DFT/6-31G/DMSO	Differ/DMSO
C1	146,74	134,81	11,93
C2	148,31	135,02	13,29
C3	152,00	133,21	18,79
C4	130,40	113,27	17,13
C5	118,21	103,52	14,69
C6	128,57	111,04	17,53
C7	115,90	101,07	14,83
C8	151,64	134,74	16,90
C9	139,71	131,85	7,86
C10	56,73	43,27	13,46
C11	164,30	153,57	10,73
C12	130,40	116,94	13,46
C13	129,56	118,15	11,41
C14	127,68	114,53	13,15
C15	130,88	118,82	12,06
C16	127,68	112,85	14,83
C17	129,56	114,36	15,20
C18	30,94	24,96	5,98
C19	134,78	120,16	14,62
C20	129,44	114,97	14,47
C21	129,09	115,03	14,06
C22	136,24	123,89	12,35
C23	129,09	114,92	14,17
C24	129,44	113,24	16,20
C25	21,06	12,27	8,79
H26	11,84	8,59	3,25
H27	9,84	11,46	-1,62

H28	7,63	8,68	-1,05
H29	7,77	8,14	-0,37
H30	7,35	7,69	-0,34
H31	3,81	4,09	-0,28
H32	3,81	4,45	-0,64
H33	3,81	4,79	-0,98
H34	8,14	9,05	-0,91
H35	7,57	8,52	-0,95
H36	7,64	8,47	-0,83
H37	7,57	8,02	-0,45
H38	8,14	8,14	0,00
H39	3,88	4,78	-0,90
H40	3,88	4,72	-0,84
H41	7,15	8,44	-1,29
H42	7,10	8,26	-1,16
H43	7,10	8,28	-1,18
H44	7,15	8,4	-1,25
H45	2,26	2,84	-0,58
H46	2,26	3,39	-1,13
H47	2,20	3,17	-0,97

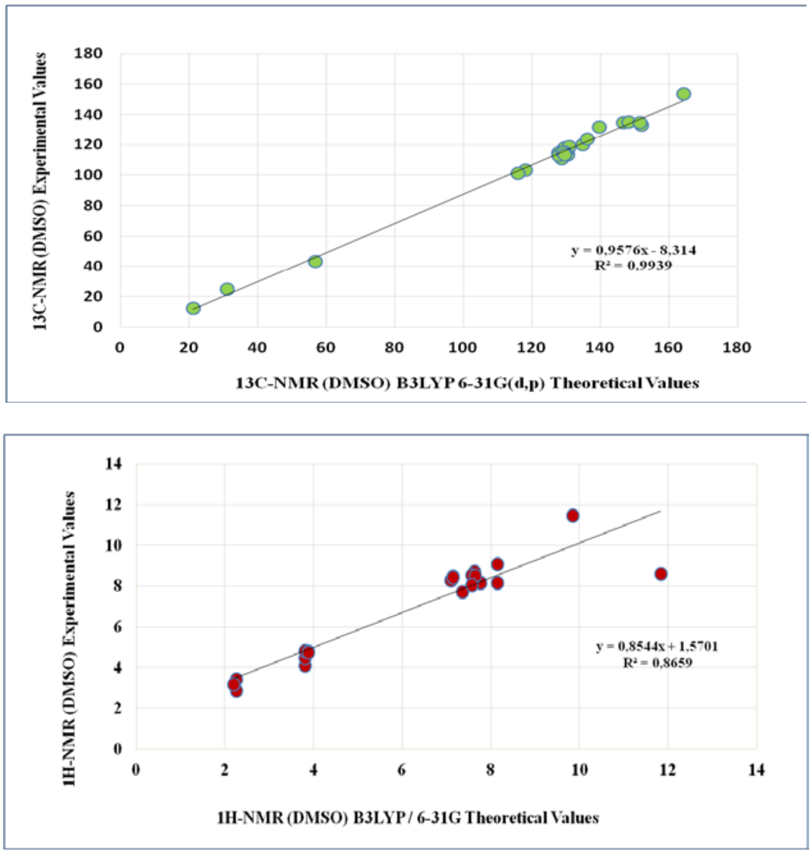

Figure 2. The experimental/ calculation ^{13}C and ^{1}H-NMR data and graps

Molecular Geometry (Bond length)

Table 2 provides a summary of the molecular geometry characteristic, bond lengths, that were estimated using DFT technique and B3LYP functional using the 6-31G (d,p) basis set. This finding indicates that the longest bond length is between C(10) and C(11) atoms, with values of 1.52 Å B3LYP 6-31G (d,p). Additionally, using the same basis sets, the bond length in the triazole ring N48-N49, N48-C1, C2-O52, C2-N50, and N50-C1 are computed as 1.38, 1.30, 1.43, 1.22, 1.38 Å respectively. The N-N, N=C, and C=O bond lengths in the literature are calculated as 1.40, 1.28, and 1.21 Å (Ocak et al., 2003; Cruz et al., 2022). The computed bond length values agree with those found in the literature. The lowest bond angle is the angle of N-H asısycproton and ıts value ıs 1.00 Å .

Table 2. The calculated Bond length

Bond length (A^0)	B3LYP	Bond length (A^0)	B3LYP
C(1)-N(48)	1.30	O(54)-C(11)	1.39
C(1)-N(50)	1.38	C(11)-O(55)	1.20
C(1)-C(18)	1.49	C(11)-C(12)	1.49
N(48)-N(49)	1.38	C(12)-C(13)	1.40
N(49)-H(26)	1.00	C(13)-H(34)	1.08
N(49)-C(2)	1.37	C(13)-C(14)	1.39
C(2)-O(52)	1.43	C(14)-H(35)	1.08
C(2)-N(50)	1.22	C(14)-C(15)	1.39
N(50)-N(51)	1.37	C(15)-H(36)	1.08
N(51)-C(3)	1.29	C(15)-C(16)	1.39
C(3)-H(27)	1.08	C(16)-H(37)	1.08
C(3)-C(4)	1.46	C(16)-C(17)	1.39
C(4)-C(5)	1.40	C(17)-H(38)	1.08
C(4)-C(9)	1.40	C(18)-H(39)	1.09
C(5)-H(28)	1.08	C(18)-H(40)	1.09
C(5)-C(6)	1.38	C(18)-C(19)	1.52
C(6)-H(29)	1.08	C(19)-C(20)	1.39
C(6)-C(7)	1.40	C(20)-H(41)	1.08
C(7)-H(30)	1.08	C(20)-C(21)	1.39
C(7)-C(8)	1.36	C(21)-H(42)	1.08
C(8)-O(53)	1.38	C(21)-C(22)	1.39
O(53)-C(10)	1.36	C(22)-C(23)	1.40
C(10)-H(31)	1.09	C(23)-H(43)	1.08
C(10)-H(32)	1.09	C(23)-C(24)	1.39
C(10)-H(33)	1.09	C(24)-H(44)	1.08
C(9)-O(54)	1.38	C(25)-H(45)	1.09
		C(25)-H(46)	1.09
		C(25)-H(47)	1.09

Mulliken Charge Data

The mulliken charges (Mulliken et al., 1955) of molecule were calculated with B3LYP 6-31 G(d,p). While the mulliken charge values of some C atoms and all protons in the molecule are positive, some C atoms and all the N48-N51, O52-O55 atoms are negative. The C2 atom, which is attached to the electronegative oxygen atom, has the highest electropositivity.

Table 3. The calculated mulliken charges

Atom	DFT	Atom	DFT
C1	0,545	H26	0,289
C2	0,815	H27	0,173
C3	0,125	H28	0,113
C4	0,035	H29	0,090
C5	-0,114	H30	0,094
C6	-0,098	H31	0.118
C7	-0,134	H32	0,118
C8	0,369	H33	0,135
C9	0,235	H34	0,107
C10	-0,081	H35	0,096
C11	0,561	H36	0,093
C12	0,037	H37	0,094
C13	-0,092	H38	0,115
C14	-0,095	H39	0,142
C15	-0,075	H40	0,130
C16	-0,096	H41	0,082
C17	-0,087	H42	0,076
C18	-0,288	H43	0,079
C19	0,124	H44	0,097
C20	-0,123	H45	0,118
C21	-0,123	H46	0,126
C22	0,125	H47	0,111
C23	-0,118	N48	-0,342
C24	-0,116	N49	-0,435
C25	-0,381	N50	-0,422
		N51	-0,318
		O52	-0,533
		O53	-0,530
		O54	-0,537
		O55	-0,428

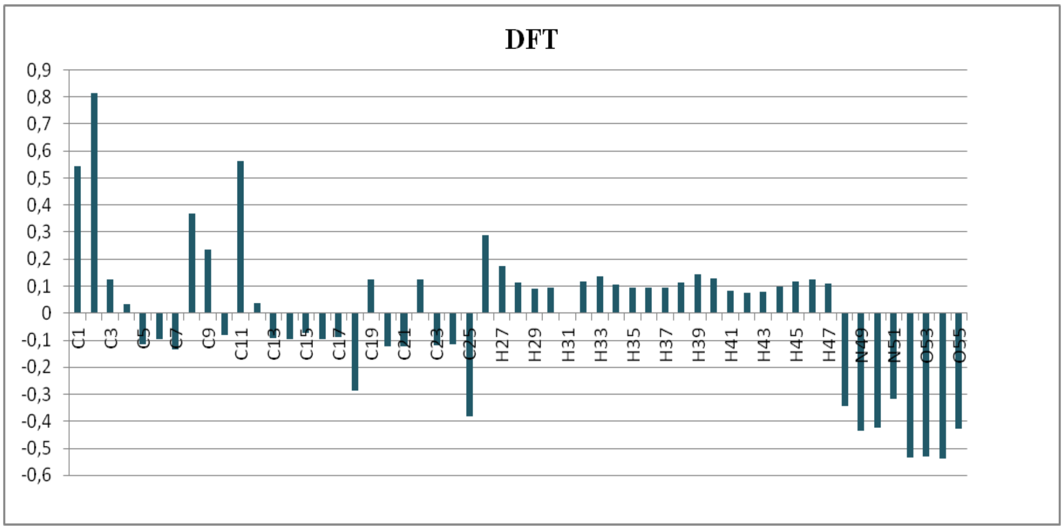

Figure 3. The calculated mulliken charges with B3LYP

FMO's Analysis

The electronic transitions, electric and optical characteristics, as well as kinetic stability, were all identified by frontier molecular orbitals (FMO) (Fukui, 1982). Three stages of calculation were used to derive the compound's HOMO-LUMO energy values, which are 4.25 eV for B3LYP basis set (figure 4). Table 4 displays the computed values for the compound's global hardness (A), electronegativity (E), chemical potential (P), softness (S), ionization potential (I), electrophilic index (E), and nucleophilic index (IP) using the E_{LUMO}-E_{HOMO} energy gap.

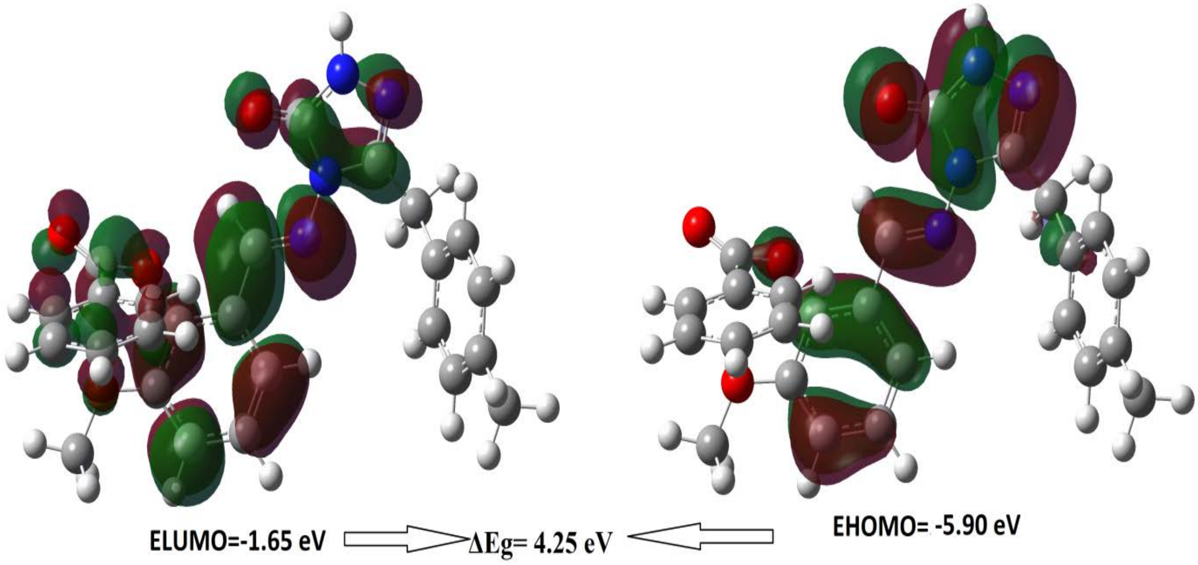

Figure 4. HOMO-LUMO and ΔEg

Table 4. The electronic parameters data of the molecule

		Hatree	ev	kcal/mol	KJ/mol
	LUMO	-0.2169	-5.902	-136.105	-569.471
	HOMO	-0.06	-1.63264	-37.6502	-157.53
A	Electron Affinity	0.2169	5.902	136.105	569.471
I	Ionization Potential	0.06	1.63264	37.6502	157.53
ΔE	Energy gap	-0.1569	-4.26936	-98.4552	-411.941
χ	electronegativity	0.13845	3.76732	86.8778	363.5
Pi	chemical potential	-0.13845	-3.76732	-86.8778	-363.5
ω	electrophilic index	-0.00075188	-0.02046	-0.47181	-1.97406
IP	Nucleophilic index	0.010861403	0.29555	6.81556	28.5166
S	molecular softness	-12.7470	-346.854	-7998.76	-33467.2
η	molecular hardness	-0.07845	-2.13468	-49.2276	-205.97

Thermodynamic Analysis

The thermodynamic parameters 298.150 K and under 1 atm pressure was used to determine using B3LYP functionals in the DFT method at 6-31G(d,p) basis set. When the thermodynamic properties that provide the formation conditions of a chemical reaction are calculated theoretically, it will be quite easy to determine the reaction conditions.

Table 5. The calculated thermodynamic properties

Rotational temperatures (Kelvin)	DFT
A	0.01568
B	0.00227
C	0.00215
Rotational constants (GHZ)	
A	0.32672
B	0.04729
C	0.04483
Thermal Energies E(kcal/mol)	
Translational	0.889
Rotational	0.889
Vibrational	267.302
Total	269.080
Thermal Capacity CV(cal/mol-K)	
Translational	2.981
Rotational	2.981
Vibrational	87.028
Total	92.989
Entropy S(cal/mol-K)	
Translational	44.149
Rotational	37.382
Vibrational	71.341
Total	152.872
Zero-point correction (Hartree/Particle)	0.407076
Thermal correction to Energy	0.428806
Thermal correction to Enthalpy	0.429750
Thermal correction to Gibbs Free Energy	0.357116
Sum of electronic and zero-point Energies	-1484.387284
Sum of electronic and thermal Energies	-1484.365554
Sum of electronic and thermal Enthalpies	-1484.364610
Sum of electronic and thermal Free Energies	-1484.437244
Zero-point vibrational energy (Kcal/mol)	255.44378

The MEP Surface Map

The relative reactivity sites in a species for nucleophilic and electrophilic attack are predicted by the molecular electrostatic potential (MEP) (Mumit et al., 2020) . By employing the optimized structure with the B3LYP/6-31G(d,p) basis set, the DFT calculation was used to calculate the MEP surface analysis of the molecule. Figure 5 shows the mapped electrostatic potential surface of the chemical under study. The chemical has a color code that ranges from -5.945e-2 to +5.945e-2. The MEP structure's red and blue colors denote regions that are more electron-rich and electron-poor, respectively. The circumference of the electronegative oxygen atoms (O52-O55) is red, while the circumference of the electropositive N49-H26 acidic proton is blue (Hussein, 2021).

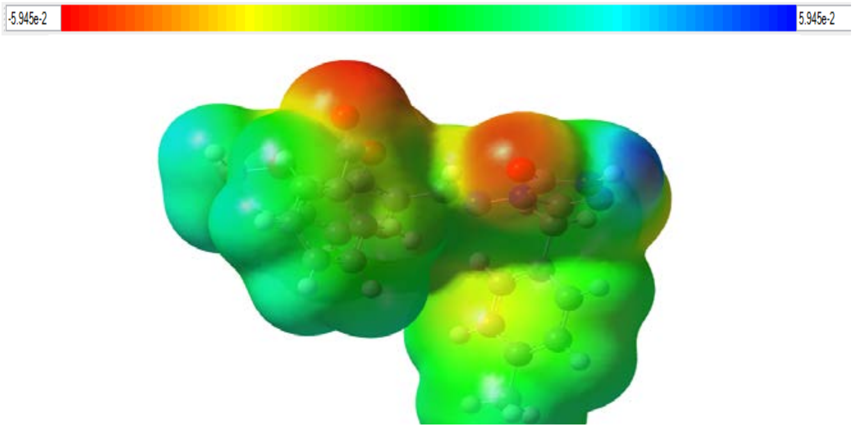

Figure 5. The MEP surface map

FT-IR Vibrational Frequency Calculations

Due to their low computational costs and typically reliable results, DFT-based computations are the most used theoretical approaches for predicting the structure through comparison of predicted and observed IR spectra. The Veda 4 software was used to acquire all FT-IR calculations (Jamroz, 2004). For the optimized structure, the vibrational frequencies were estimated at the B3LYP/ 6-31G(d,p) level of theory and scaled by 0.9617 (Merrick et al., 2007). The scaled infrared values and experimental values were compared, and the results are shown in Table 6.

Table 6**.** The theoretical and calculated infrared data

vibrational frequencies	Experimental IR	Scaled B3LYP
ν (NH)	3189	3556
ν (C=O)	1746, 1709	1774, 1756
ν (C=N)	1551	1609
ν (COO)	1259	1278
1,4-Disubstituted-benzene	803	806

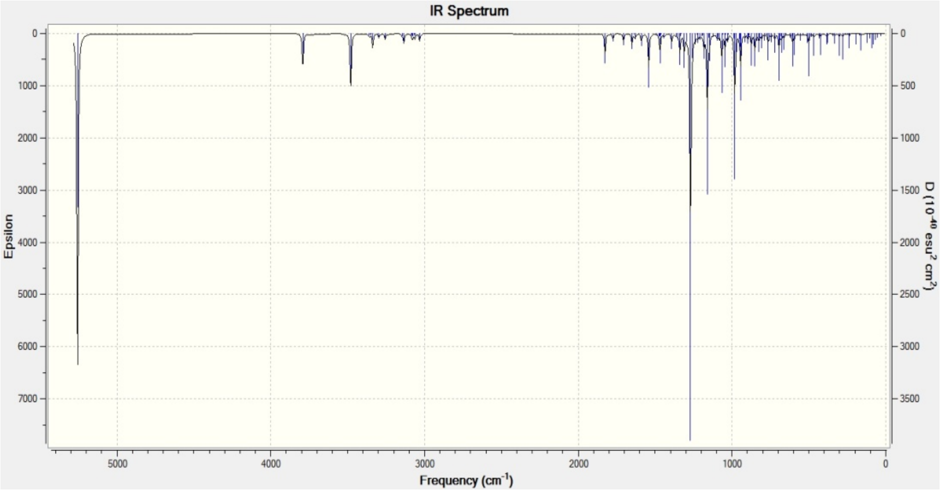

Figure 6. The IR Spectrum with DFT(B3LYP)

NLO Analysis

Electromagnetic field interactions can have an impact on non-linear optical (NLO) characteristics in a variety of contexts. For technologies in fields like telecommunications, signal processing, and optical interactions, NLO features are crucial for supplying the essential tasks of frequency shifting, optical modulation, optical switching, optical logic, and optical memory (Bitmez et al., 2014). NLO is thus situated at the cutting edge of current research. The energy of the highest occupied molecular orbital (E_{HOMO}), energy of the lowest unoccupied molecular orbital (E_{LUMO}), and energy gap between the LUMO and HOMO (EGAP) are some quantum chemical parameters that have been used to explain NLO properties. These parameters include the total static dipole moment (μ), average linear polarizability (α), anisotropy of polarizability ($\Delta\alpha$), and first hyperpolarizability (β_{total}). Another crucial factor in determining the NLO qualities is E_{HOMO}. A high value of E_{HOMO} reflects a molecule's propensity for electron transfer to a low unoccupied molecular orbital. A low E_{LUMO} value suggests that a molecule has a larger capacity for receiving electrons. The NLO characteristics of the examined compounds rise when HOMO and LUMO energy levels rise and fall, respectively (Sayin et al., 2015). In results the calculations DFT 6-31G(d,p), Polar (αxx, αxy, αyy, αxz ,αyz, αzz)= 372.4922748, 21.2118185, 308.2578439, 18.4087961, 1.6380612, 236.225101; HyperPolar (βxxx, βxxy, βxyy, βyyy, βxxz, βxyz, βyyz, βxzz, βyzz, βzzz)= 94.8132254, -277.5042246, -159.574997, -227.6931422, -62.1540947, -77.2269366, -84.2142141, -23.6395059, 7.2111351, -59.7315603, respectively were obtained. The theoretical results are α_{total}: 45.299 x10^{-24} esu, $\Delta\alpha$: 16.168 x10^{-24} esu, and β^0 : 45.71 x10^{-31} esu. The primary reference material for NLO qualities is the urea molecule. According to published data, the NLO parameters are: α_{total}: 5.07643717x10^{-24} esu, $\Delta\alpha$: 2.13568262x10^{-24} esu, and β^0 : 7.2228469891x10^{-31} esu (Kotan et al., 2020). The NLO values were 9, 8, and 6.5 times more than ur ea as compared to the reference material.

Table 7. The total energy $\mathbf{E_{total}}$ (Hatree), the electric dipole moment $\boldsymbol{\mu}$ (D), the average polarizability $\boldsymbol{\alpha_{total}}$ (10^{-24} esu) and first hyperpolarizability $\boldsymbol{\beta_{total}}$ (10^{-31} esu) of molecule.

	B3LYP
E_{total}	-1485,81197087
μx	2,7208
μy	8,1260
μz	-3,8837
μToplam	9,4084
αxx	372,4922748
αxy	21,2118185
αyy	308,2578439
αxz	18,4087961
αyz	1,6380612
αzz	236,225101
α_{total}	45.299 $x10^{-24}$ esu
Δα (esu)	16.168 $x10^{-24}$ esu
βxxx	94,8132254
βxxy	-277,5042246
βxyy	-159,574997
βyyy	-227,6931422
βxxz	-62,1540947
βxyz	-77,2269366
βyyz	-84,2142141
βxzz	-23,6395059
βyzz	7,2111351
βzzz	-59,7315603
β_{total}	45.71 $x10^{-31}$ esu

Conclusion

This theoretical effort used DFT (B3LYP) calculations to determine the target molecule using the 6-31G(d,p) basis sets using the Gaussian G09W software package. The calculations' ^{1}H chemical shifts and FT-IR data are observed to be in agreement with the actual data. The R2 values showed a linear association, while the H-NMR correlation graph shows a minor divergence. The N-H acidic proton (H26) in the molecule is the cause of this divergence. The sole explanation for the infrared data's lack of negative frequency is the molecule's stability. The ΔEg value was calculated as 4.25 eV. Regions that are electrophilic and nucleophilic were identified using MEP analysis. As a result of NLO analysis, the molecule was found to be a good nonlinear substance.

Scientific Ethics Declaration

The authors declare that the scientific ethical and legal responsibility of this article published in EPSTEM journal belongs to the authors.

Acknowledgements or Notes

* This article was presented as an oral presentation at the International Conference on Basic Sciences and Technology (www.icbast.net) held in Antalya/Turkey on November 16-19, 2022.

References

Abuo-Rahma, G. E. D. A., Abdel-Aziz, M., Farag, N. A., & Kaoud, T. S. (2014). Novel 1-[4-(Aminosulfonyl) phenyl]-1H-1, 2, 4-triazole derivatives with remarkable selective COX-2 inhibition: Design, synthesis, molecular docking, anti-inflammatory and ulcerogenicity studies. *European Journal of Medicinal Chemistry*, *83*, 398-408.

Aly, A. A., A. Hassan, A., Makhlouf, M. M., & Bräse, S. (2020). Chemistry and biological activities of 1, 2, 4-triazolethiones antiviral and anti-infective drugs. *Molecules*, *25*(13), 3036.

Beytur, M., & Avinca, I. (2021). Molecular, electronic, nonlinear optical and spectroscopic analysis of heterocyclic 3-substituted-4-(3-methyl-2-thienylmethyleneamino)-4, 5-dihydro-1h-1, 2, 4-triazol-5-ones: experiment and dft calculations. *Heterocyclic Communications*, *27*(1), 1-16.

Bitmez, Ş., Sayin, K., Avar, B., Köse, M., Kayraldız, A., & Kurtoğlu, M. (2014). Preparation, spectral, X-ray powder diffraction and computational studies and genotoxic properties of new azo–azomethine metal chelates. *Journal of Molecular Structure*, *1076*, 213-226.

Boy, S., Aras, A., Türkan, F., Akyıldırım, O., Beytur, M., Sedef Karaman, H., & Yüksek, H. (2021). Synthesis, Spectroscopic Analysis, and in Vitro/in Silico Biological Studies of Novel Piperidine Derivatives Heterocyclic Schiff‐Mannich Base Compounds. *Chemistry & Biodiversity*, *18*(12), 2100433.

Cruz, J., Garcia-Ochoa, E., & Castro, M. (2002). Experimental and theoretical study of the 3-amino-1, 2, 4-triazole and 2-aminothiazole corrosion inhibitors in carbon steel. *Journal of The Electrochemical Society*, *150*(1), B26.

Dharmaraj, N., Viswanathamurthi, P., & Natarajan, K. (2001). Ruthenium (II) complexes containing bidentate Schiff bases and their antifungal activity. *Transition Metal Chemistry*, *26*(1), 105-109.

Frisch, A., Nielson, A.B., & Holder, A.J. (2003). *Gaussvıew User Manual, Gaussian*, Inc., Wallingford, CT.

Fukui, K. (1982). Role of frontier orbitals in chemical reactions. *science*, *218*(4574), 747-754.

Gao, F., Wang, T., Xiao, J., & Huang, G. (2019). Antibacterial activity study of 1, 2, 4-triazole derivatives. *European Journal of Medicinal Chemistry*, *173*, 274-281.

Gürbüz, A., Alkan, M., Manap, S., Özdemir, G., Yüksek, H., (2021). Synthesıs and antimicrobial activities of novel 2- methoxy-6-[(3-(p-methylbenzyl)-4,5-dihydro-1h-1,2,4-triazol-5-one-4-yl)-azomethin]-phenyl benzoates with their nonaqueous medium titrations". *World Journal of Pharmacy and Pharmaceutical Sciences, Wjpps*, *10*(9), 65-80.

Hussein, R. K., Elkhair, H. M., Elzupir, A. O., & Ibnaouf, K. H. (2021). Spectral, structural, stability characteristics and frontier molecular orbitals of tri-n-butyl phosphate (tbp) and its degradation products: DFT calculations. *J. Ovonic Res*, *17*, 23-30.

Jamróz, M.H. (2004). Vibrational energy distribution analysis: VEDA 4 program, Warsaw.

Jin, R. Y., Zeng, C. Y., Liang, X. H., Sun, X. H., Liu, Y. F., Wang, Y. Y., & Zhou, S. (2018). Design, synthesis, biological activities and DFT calculation of novel 1, 2, 4-triazole Schiff base derivatives. *Bioorganic Chemistry*, *80*, 253-260.

Kaproń, B., Czarnomysy, R., Wysokiński, M., Andrys, R., Musilek, K., Angeli, A., & Plech, T. (2020). 1, 2, 4-Triazole-based anticonvulsant agents with additional ROS scavenging activity are effective in a model of pharmacoresistant epilepsy. *Journal of Enzyme Inhibition and Medicinal Chemistry*, *35*(1), 993-1002.

Kotan, G. (2021). Novel mannich base derivatives: Synthesis, characterization, antimicrobial and antioxidant activities. *Letters in Organic Chemistry*, *18*(10), 830-841.

Kotan, G., Gökce, H., Akyıldırım, O., Yüksek, H., Beytur, M., Manap, S., & Medetalibeyoğlu, H. (2020). Synthesis, spectroscopic and computational analysis of 2-[(2-Sulfanyl-1H-benzo [d] imidazol-5-yl) iminomethyl] phenyl naphthalene-2-sulfonate. *Russian Journal of Organic Chemistry*, *56*(11), 1982-1994.

Kotan, G., Manap, S., & Yüksek, H. (2022). Synthesis, characterization, antioxidant and DFT studies of some novel Schiff base compounds. *Journal of Computational Biophysics and Chemistry*, *21*(1), 47-63.

Merrick J.P., Moran D., & Radom L. (2007). An evaluation of harmonic vibrational frequency scale factors. *Journal of Physical Chemistry*, *111*(45), 11683-11700.

Mulliken, R. S. (1955). Electronic population analysis on LCAO–MO molecular wave functions. I. *The Journal of Chemical Physics*, *23*(10), 1833-1840.

Mumit, M. A., Pal, T. K., Alam, M. A., Islam, M. A. A. A. A., Paul, S., & Sheikh, M. C. (2020). DFT studies on vibrational and electronic spectra, HOMO–LUMO, MEP, HOMA, NBO and molecular docking analysis of benzyl-3-N-(2, 4, 5-trimethoxyphenylmethylene) hydrazinecarbodithioate. *Journal of molecular structure*, *1220*, 128715.

Ocak, N., Çoruh, U., Kahveci, B., Şaşmaz, S., Vazquez-Lopez, E. M., Erdönmez, A. (2003). 1-Acetyl-3-(p-chlorobenzyl)-4-(p-chlorobenzylidenamino)-4,5-dihydro-1*H*-1,2,4-triazol-5-one. *Acta Cryst. Sec. E.,* 59(6), 750-752.

Patel, V. M., Patel, N. B., Chan-Bacab, M. J., & Rivera, G. (2018). Synthesis, biological evaluation and molecular dynamics studies of 1, 2, 4-triazole clubbed Mannich bases. *Computational Biology and Chemistry*, *76*, 264-274.

Qiao, X., Ma, Z. Y., Xie, C. Z., Xue, F., Zhang, Y. W., Xu, J. Y., ... & Yan, S. P. (2011). Study on potential antitumor mechanism of a novel Schiff Base copper (II) complex: synthesis, crystal structure, DNA binding, cytotoxicity and apoptosis induction activity. *Journal of Inorganic Biochemistry*, *105*(5), 728-737.

Sayin, K., Karakaş, D., Karakuş, N., Sayin, T. A., Zaim, Z., & Kariper, S. E. (2015). Spectroscopic investigation, FMOs and NLO analyses of Zn (II) and Ni (II) phenanthroline complexes: A DFT approach. *Polyhedron*, *90*, 139-146.

Shi, J., Ding, M., Luo, N., Wan, S., Li, P., Li, J., & Bao, X. (2020). Design, synthesis, crystal structure, and antimicrobial evaluation of 6-fluoroquinazolinylpiperidinyl-containing 1, 2, 4-triazole Mannich base derivatives against phytopathogenic bacteria and fungi. *Journal of Agricultural and Food Chemistry*, *68*(36), 9613-9623.

Singla, N. (2020). Synthetic and medicinal attributes of 1, 2, 4-triazole derivatives. *Annals of Tropical Medicine and Public Health*, *23*, 231-541.

Wolinski, K., .Hilton, J. F., Pulay, P. J. (1990). Efficient implementation of the gauge-independent atomic orbital method for NMR chemical shift calculations. *Journal of the American Chemical Society*, *112*, 512.

Yiğit, B., Yiğit, M., Taslimi, P., Gök, Y., & Gülçin, İ. (2018). Schiff bases and their amines: Synthesis and discovery of carbonic anhydrase and acetylcholinesterase enzymes inhibitors. *Archiv der Pharmazie*, *351*(9), 1800146.

Yüksek, H., Göksu, B., Manap, S., Beytur, M., & Gürsoy Kol, Ö. (2018). Synthesis of some new 4-[2-(2-methylbenzoxy)-benzylidenamino]-4, 5-dihydro-1H-1, 2, 4-triazol-5-one derivatives with their antioxidant properties. *Int J Chem*, *22*(2), 1-29.

Yüksek, H., Özdemir, G., Manap, S., Yılmaz, Y., Kotan, G., Gürsoy-Kol, Ö., & Alkan, M. (2020). Synthesis and ınvestigations of antimicrobial, antioxidant activities of novel di-[2-(3-alkyl/aryl-4, 5-dihydro-1h-1, 2, 4-triazol-5-one-4-yl)-azomethinephenyl] isophtalates and mannich base derivatives. *ACTA Pharmaceutica Sciencia, 58*(1).

Yüksek, H., Özdemir, G., Manap, S., Yılmaz, Y., Kotan, G., Gürsoy-Kol, Ö., & Alkan, M. (2020). Synthesis and Investigations of antimicrobial, antioxidant activities of novel di-[2-(3-alkyl/aryl-4, 5-dihydro-1h-1, 2, 4-triazol-5-one-4-yl)-azomethinephenyl] ısophtalates and mannich base derivatives. *ACTA Pharmaceutica Sciencia*, *58*(1).

Author Information

Gul Kotan	**Haydar Yuksek**
Kafkas University	Kafkas University
Kafkas University, Kars Vocational School, Kars, Turkey	Faculty of Science and Letters, Department of Chemistry, Kars, Turkey
Contact E-mail: *gulkemer@hotmail.com*	

To cite this article:

Kotan, G. & Yüksek, H. (2022). Theoretical (B3lyp) and spectroscopic (ft-ır, ^{1}h-nmr and ^{13}c-nmr) investigation of 2- methoxy-6-[(3-(*p*-methylbenzyl)-4,5-dihydro-1*h*-1,2,4-triazol-5-one-4-yl)-azomethin]-phenyl benzoate. *The Eurasia Proceedings of Science, Technology, Engineering & Mathematics (EPSTEM), 20,* 84-93.